

# A high energy-resolution zero degree facility for (p,p') and (p,t) reactions

R Neveling<sup>1</sup>, H Fujita<sup>2</sup>, FD Smit<sup>1</sup>, T Adachi<sup>3</sup>, GPA Berg<sup>4</sup>, EZ Buthelezi<sup>1</sup>, J Carter<sup>5</sup>, JL Conradie<sup>1</sup>, M Couder<sup>4</sup>, RW Fearick<sup>6</sup>, SV Förtsch<sup>1</sup>, D Fourie<sup>1</sup>, Y Fujita<sup>7</sup>, J Görres<sup>4</sup>, K Hatanaka<sup>2</sup>, AM Heilmann<sup>8</sup>, JP Mira<sup>1</sup>, SHT Murray<sup>1</sup>, P von Neumann-Cosel<sup>8</sup>, S O'Brien<sup>4</sup>, P Papka<sup>1,9</sup>, I Poltoratska<sup>8</sup>, A Richter<sup>8,10</sup>, E Sideras-Haddad<sup>5</sup>, JA Swartz<sup>9</sup>, A Tamii<sup>7</sup>, IT Usman<sup>1</sup> and JJ van Zyl<sup>9</sup>

<sup>1</sup> iThemba Laboratory for Accelerator Based Sciences, Somerset West 7129, South Africa

<sup>2</sup> Research Center for Nuclear Physics, Osaka University, Ibaraki, Osaka 560-0047, Japan

<sup>3</sup> KVI, Zernikelaan 25, 9747 AA Groningen, The Netherlands

<sup>4</sup> Department of Physics and the Joint Institute for Nuclear Astrophysics, University of Notre Dame, Notre Dame, Indiana 46556, USA

<sup>5</sup> School of Physics, University of Witwatersrand, Johannesburg 2050, South Africa

<sup>6</sup> Physics Department, University of Cape Town, Rondebosch 7700, South Africa

<sup>7</sup> Department of Physics, Osaka University, Toyonaka, Osaka 560-0043, Japan

<sup>8</sup> Institut für Kernphysik, Technische Universität Darmstadt, D-64829, Darmstadt, Germany

<sup>9</sup> Department of Physics, University of Stellenbosch, Matieland 7602, South Africa

<sup>10</sup> ECT\*, Villa Tambosi, I-38123 Villazano (Trento), Italy

E-mail: [neveling@tllabs.ac.za](mailto:neveling@tllabs.ac.za)

**Abstract.** Medium-energy hadronic scattering and reactions at zero degrees are very selective to excitations with low angular momentum transfer. Only a few facilities exist worldwide where high energy-resolution measurements of this nature can be performed. The K600 Zero-Degree Facility at iThemba LABS, South Africa, was recently successfully developed. Measurements were performed for inelastic proton scattering at an incident energy of 200 MeV for targets ranging from <sup>27</sup>Al to <sup>208</sup>Pb. Excitation energy-resolution of 50 keV (FWHM) was achieved. A reasonable background subtraction procedure allows for the extraction of excitation energy spectra with low background. Measurements of the (p,t) reaction at 100 MeV benefit from a large difference in magnetic rigidity between the reaction products and primary particles, resulting in almost background-free spectra with excitation energy-resolution of 32 keV (FWHM).

## 1. Introduction

The investigation of medium-energy hadronic scattering and reactions at zero degrees (0°) has the advantage of being very selective to excitations with low angular momentum transfer. This simplifies the analysis of the many contributions to the spectra due to the complex nature of the nuclear interaction. Only a few facilities exist worldwide where high energy-resolution measurements of this nature can be performed by separating the primary beam from the inelastically scattered particles or reaction products by means of a magnetic spectrometer [1]. At the Research Center for Nuclear Physics (RCNP), Osaka, Japan, the (<sup>3</sup>He,t) reaction has

been established as a tool for the determination of Gamow-Teller (GT) strengths from (p,n)-type reactions, reaching an energy-resolution of  $\sim 25$  keV (FWHM) at 140 MeV/nucleon [2]. High energy-resolution studies into the level structure of unstable nuclei of astrophysical importance have also been performed at RCNP by employing the (p,t) two neutron pickup reaction [3]. At the Kernfysisch Versneller Instituut (KVI), Groningen, Netherlands, measurements with energy-resolution of approximately 100 keV (FWHM) were successfully made with the (n,p)-type (d, $^2\text{He}$ ) reaction at  $E_d=183.5$  MeV as a measure of  $\text{GT}_+$  strengths [4, 5].

High energy-resolution measurements of (p,p') inelastic scattering  $0^\circ$  present an even more difficult experimental challenge, as the difference in magnetic rigidity between the projectiles and scattered particles is smaller than for the above-mentioned reactions. Studies of the (p,p') reaction at energies of a few hundred MeV and at  $0^\circ$  permit the extraction of complete electric dipole strength distributions (via the relativistic Coulomb excitation). This can provide, for instance, important information about the nature of the pygmy dipole resonance (PDR), a soft E1 mode at energies well below the isovector giant dipole resonance (see e.g. [6, 7] and Refs. therein). Zero degree (p,p') experiments can also be used for studies of spin-M1 strength distributions, where quenching is still an unresolved issue [8].

Until now, high energy-resolution inelastic proton scattering at  $0^\circ$  and at intermediate energies was successfully measured only at two laboratories, namely with the (now decommissioned) K=600 magnetic spectrometer at the Indiana University Cyclotron Facility (IUCF), Indiana, USA [9, 10], and with the Grand Raiden magnetic spectrometer at RCNP [1]. This paper reports the recent successful development of another high energy-resolution  $0^\circ$  facility and first successful investigations of the (p,p') and (p,t) reactions at intermediate energies at the iThemba Laboratory for Accelerator Based Sciences (iThemba LABS), South Africa.

## 2. Experimental setup

The iThemba LABS K=600 QDD magnetic spectrometer consists of five active elements namely a quadrupole magnet, two dipole magnets and two trim coils (K and H) as shown in Fig. 1. According to the original design the momentum dispersion along the focal plane can be varied between the nominal values of 6.2 cm/% and 9.8 cm/% by varying the ratio of the fields of the two dipole magnets D1 and D2, resulting in three distinct possible focal planes as indicated in Fig. 1. Vertical focusing at the focal plane is achieved with the quadrupole magnet at the entrance of the spectrometer. The two trim coils, which are shaped pole face current windings located inside the dipoles, are used to achieve the final focusing at the focal-plane. The K-coil, a quadrupole focusing element, is used to compensate for first-order kinematic variations of momentum with angle  $\theta$  in the scattering plane. The H-coil, a hexapole focusing element, is used to correct for ( $x \mid \theta^2$ ) aberrations.

During (p,p') measurements at  $0^\circ$  both the primary beam and scattered particles pass through the spectrometer. The beam passes only 10 cm from the edge of the sensing region of the focal plane detectors, positioned in the high dispersion focal plane. Of the three focal planes available this particular one is selected as a high dispersion is desired for good separation of the beam from the lowest measurable excitation energy  $E_x$  [11]. This enables access to smaller excitation energies than would be possible with the other focal planes. From the spectrometer the beam is transported through the  $0^\circ$  beam line to the Faraday cup embedded in the concrete wall of the experimental area.

In contrast to (p,p') reactions, the ground state is accessible in the study of (p,t) reactions. Due to the difference in rigidity between the beam and the particles of interest the proton beam is collected at an L-shaped brass beam-stop placed inside the first dipole of the spectrometer, indicated in Fig. 1, while the tritons are focused on the medium dispersion focal plane. This focal plane can cover a bigger momentum range, which allows for investigation of a broad excitation energy region (as required in the initial (p,t) experiments) with fewer spectrometer field-sets.

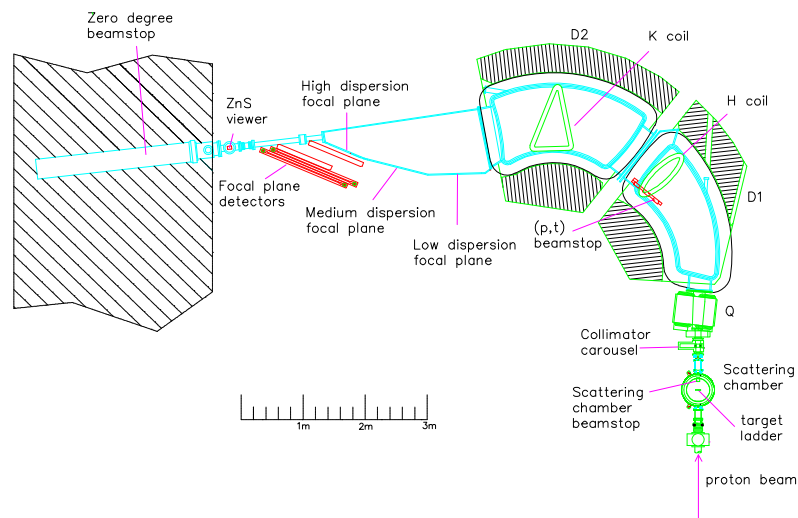


**Figure 1.** A schematic overview of the K600 magnetic spectrometer in the  $0^\circ$  mode. The focal plane detectors are shown positioned in the high dispersion focal plane. The (p,t) beam-stop in D1 is removed during (p,p') measurements.

Reaction products are observed with position sensitive focal plane detectors, consisting of two multi-wire drift chambers (MWDC) and two  $121.92 \times 10.16 \text{ mm}^2$  plastic scintillators, respectively 12.7 mm and 6.35 mm thick in the case of (p,p') measurements and 3.175 mm and 12.7 mm thick in the case of the lower energy (p,t) measurements. Each MWDC has two wire-planes, namely an X wire-plane with wires perpendicular to the scattering plane, and a U wire-plane with wires angled at  $50^\circ$  with respect to the scattering plane. The wire-planes consist of gold-plated tungsten signal-wires, 20  $\mu\text{m}$  in diameter, spaced 4 mm apart. Interspersed between these wires at equal distances are field shaping wires made of 50  $\mu\text{m}$  diameter gold-plated tungsten. The horizontal position resolution of the X wire-planes is  $\sim 0.35 \text{ mm}$  (FWHM) for a typical 5-wire event. By combining information from the X and U wire-planes the vertical position can be determined with a position resolution of  $\sim 0.8 \text{ mm}$  (FWHM). Typical individual wire-plane efficiency is 92%, with an overall tracking efficiency of 71%.

### 3. Experimental method

High energy-resolution measurements at or close to  $0^\circ$  demand beam delivery subject to stringent requirements. The ion source, injector and main accelerator, the Separated Sector Cyclotron (SSC), as well as the transfer beam line elements up to the object slit (the object point for the high energy transfer beam line ion optical system) must be set up to minimize beam energy-spread, emittance and halo. Furthermore, a small horizontal beam size at the object point is a necessary condition for high energy-resolution in the spectrometer focal plane [12]. The high energy transfer beam lines between the object point and the target must then be set up to achieve dispersion matching conditions between the beam line and the magnetic spectrometer.

The transmission efficiency of the SSC for a 100 MeV proton beam can reach 95%. However, at  $E_p=200 \text{ MeV}$  the SSC transmission efficiency is only 50-60%. The deterioration in transmission for the increase in beam energy can be attributed to the beam emittance limitations of the accelerator complex. The absence of available mechanisms to decrease the emittance, such as flat topping in the accelerators, necessitates beam setup procedures that differ from established  $0^\circ$  techniques used with great success at RCNP [1]. The most striking difference

concerns the use of horizontal and vertical slits to define the size of the beam at the object point to 1 mm in width and 2 mm in height. In addition, the beam divergence and energy spread are defined by hardware slits downstream of the object point. The result is that for  $E_p=100$  MeV only 80% of the beam extracted from the SSC reaches the target while for  $E_p=200$  MeV the throughput is much lower at 8%. In spite of these significant beam intensity losses, which are clearly potential sources of beam halo, the combination of a thin-lipped object slit, two  $90^\circ$  bending magnets and four sets of clean-up slits, both horizontal and vertical, in the high energy transfer beam lines ensures that relatively low beam halo conditions can be achieved.

In order to improve clean transmission through the spectrometer in the (p,p') case, a dipole ratio  $R=B(D1)/B(D2)=1.49$  is used which is higher than the designed ratio for the high dispersion mode ( $R=1.33$ ). This has the added advantage of increasing the dispersion from the designed 9.8 cm/% to 10.9 cm/%. The (p,p') background count-rates in the focal plane detectors can be optimized to acceptable levels of  $\sim 100$  Hz per nA after careful tuning of the beam on empty target frame. In addition to the beam halo another component of the background is observed once the empty target frame is replaced by the target foils. This background, found to increase with an increase in target mass, results from small angle elastic scattering off the target followed by re-scattering off any exposed part inside the spectrometer [9]. Furthermore, it is found that this *target related* background (as opposed to beam halo or beam related background) is sensitive to the geometry of the collimator that defines the spectrometer acceptance. The lowest background condition is achieved with a 49 mm diameter collimator which has a 11 mm thick brass lip tapered to the angular acceptance, which corresponds to a vertical and horizontal angular acceptance of  $\pm 1.91^\circ$ .

The considerable background initially observed for the (p,t) reaction at  $0^\circ$  is related to the presence of the beam-stop in D1. Slight changes of the location of the beam-stop as well as the re-positioning of the spectrometer at a small non-zero angle ( $-1.2^\circ$ ) lowers the background considerably. Note that the spectrometer angle is however still small enough to include  $0^\circ$  in the angular acceptance. Under these conditions the energy-loss characteristics of the background in the scintillators, combined with the character of the relative time of flight (TOF) of the background, measured between the SSC RF signal and the scintillator trigger, makes it possible to clearly distinguish between triton and background events. Therefore it is possible to utilize the off-focus ion optical mode of the spectrometer, which enables the determination of the vertical component of scattering angles from vertical position measurements in the focal plane [13]. By increasing the quadrupole current to 15% above its nominal medium dispersion mode setting, thereby changing to over-focus mode, the particles are spread vertically across  $\sim 70$  mm in both drift chambers.

The dispersion matched condition is achieved by using the faint beam method [12] whereby the beam intensity is lowered from a few nA to a few hundred protons per second. This is achieved by utilizing beam attenuation meshes installed between the ion source and the injector cyclotron. By scaling the five spectrometer magnetic elements proportionally to allow the proton beam to pass through the focal plane detectors one can make a direct measurement of the degree of dispersion matching achieved. The beam line elements are then optimized in order to minimize the size of the beam image in the  $(x_{fp}, \theta_{fp})$  scatter-plot. Lateral dispersion and focus matching is thus achieved, resulting in a faint beam energy-resolution of 30 keV (FWHM) at 200 MeV and 25 keV (FWHM) at 100 MeV. Unfortunately suitable beam line elements are not yet available to obtain an angular dispersion matched condition, resulting in ambiguities in the determination of the horizontal component of the scattering angle.

#### 4. Results

The reduction and subtraction of background are potentially challenging tasks in the case of (p,p') measurements. While the majority of the beam halo events can be distinguished from the

physics events through differences in TOF, the more problematic target related background has energy loss and TOF characteristics that are very similar to that of the physics events. Hence the spectrometer is operated in the vertically focused mode to distinguish physics events, focused around  $y_{fp} = 0$ , from background events which are evenly distributed in the vertical direction. The distribution of events in the focal plane is shown in the 2D scatter-plot in Fig. 2. Background subtraction is performed by assuming that the shape of the background underneath the central region can be approximated by two  $\Delta y$  regions on either side, each vertically half the size of the central region. The bottom plot in Fig. 2 illustrates the focal plane position spectrum for all events in the central region and the background that results from the sum of the two outer  $\Delta y$  sections. The focal plane region within the horizontal position range  $710 \text{ mm} \leq x_{fp} \leq 800 \text{ mm}$  represents the portion of the MWDC that is in the shadow of the vacuum chamber wall between the  $0^\circ$  beam line and the high momentum dispersion focal plane exit window. The difference between the central and background sections results in a reasonably background-free spectrum, as illustrated in the calibrated excitation energy spectra in Fig. 3. This figure represents two of the five target nuclei (including  $^{208}\text{Pb}$ ) which were successfully investigated. The accessible excitation energy range is from 8.5 MeV to 24.5 MeV, which corresponds to a momentum range of  $0.931\text{-}0.976 P_p$ , where  $P_p$  is the momentum of the proton beam. An energy resolution of 50 keV (FWHM) is achieved.

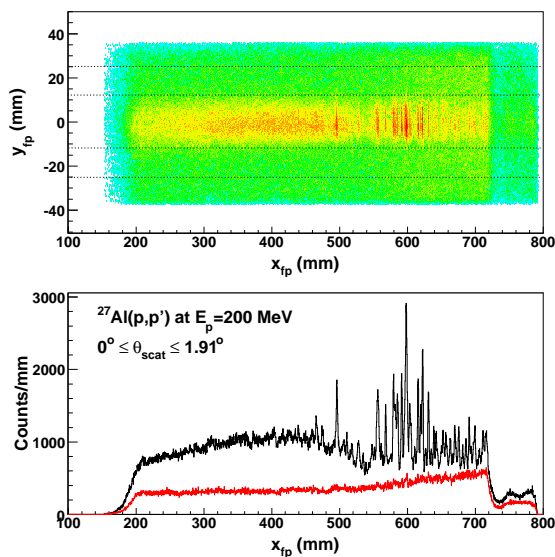


**Figure 2.** Top:  $(x_{fp}, y_{fp})$  distribution of events for the  $^{27}\text{Al}(p,p')$  reaction. Bottom: Focal plane position for the  $^{27}\text{Al}(p,p')$  reaction for the central  $\Delta y$  region (black line) and the background obtained from the sum of the two outer  $\Delta y$  sections (red line).

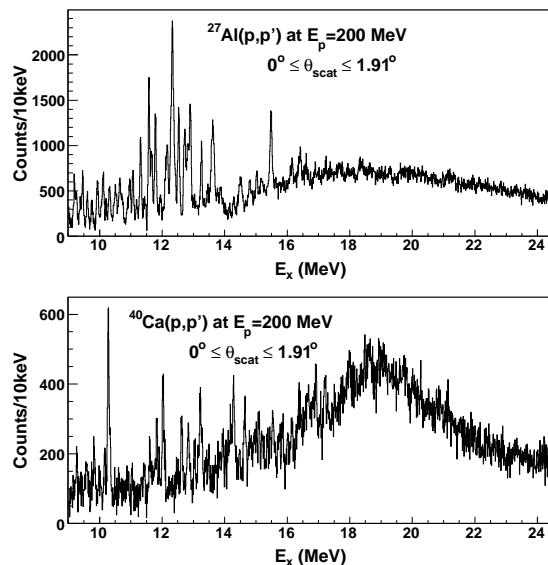


**Figure 3.** Experimental excitation energy spectra for inelastic proton scattering at  $0^\circ$  from  $^{27}\text{Al}$  and  $^{40}\text{Ca}$  at  $E_p = 200 \text{ MeV}$ , after background subtraction as illustrated in Fig.2.

In the case of (p,t) measurements no background subtraction is required since particle identification (PID) methods allows one to clearly distinguish the tritons from the background. The off-focus character of the ion optics is clearly visible in Fig. 4, where the  $(x_{fp}, y_{fp})$  distribution of events is shown for  $-2^\circ \leq \theta_{scat} \leq 2^\circ$  and  $-1^\circ \leq \phi_{scat} \leq 2^\circ$ . The experimental energy-resolution of 32 keV (FWHM) is achieved following software corrections for a slight linear dependence of the focal plane position on the horizontal scattering angle. The accessible excitation energy range for the spectrometer field-set which includes the ground state is

approximately from 0 to 11 MeV. Measurements for a second field-set can also be made for the proton beam stopping in the same beam-stop in D1. This extends the measurement to  $E_x=15.5$  MeV while allowing for ample overlap with the first field-set. Calibrated excitation energy spectra for both field-sets of the  $^{40}\text{Ca}(p,t)$  reaction are shown in Fig. 5 for angles smaller than  $\theta_{lab}=1^\circ$ . The estimated scattering angle resolution is  $0.6^\circ$  (FWHM).

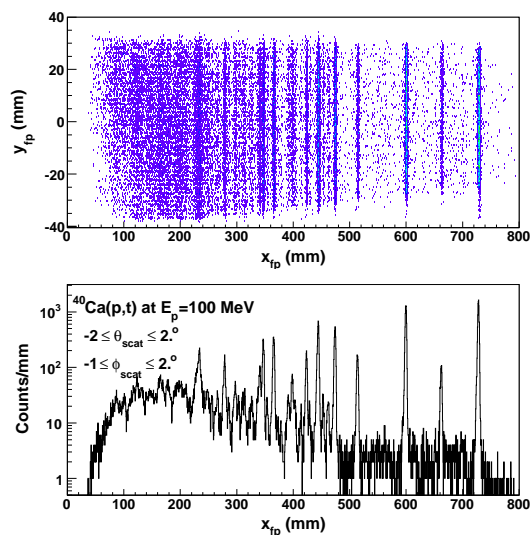


**Figure 4.** Top:  $(x_{fp}, y_{fp})$  distribution of events for the  $^{40}\text{Ca}(p,t)$  reaction. Bottom: Focal plane position spectrum for the  $^{40}\text{Ca}(p,t)$  reaction. Both histograms are for the angular acceptance  $-2^\circ \leq \theta_{scat} \leq 2^\circ$  and  $-1^\circ \leq \phi_{scat} \leq 2^\circ$ .

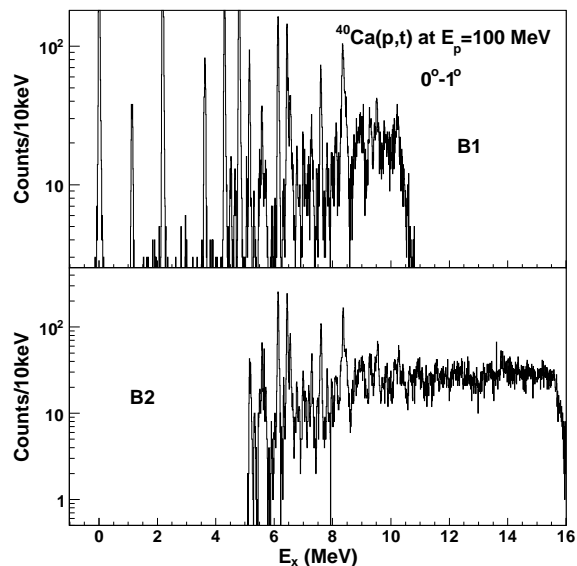


**Figure 5.** Excitation energy spectrum of the  $^{40}\text{Ca}(p,t)$  reaction at 100 MeV for angles smaller than  $1.0^\circ$  for the field-sets that include the ground state (B1) and the higher excitation energy region up to 15.5 MeV (B2).

## Acknowledgments

We are indebted to the accelerator staff at iThemba LABS for providing excellent beams. We also thank Franz Gonglach for technical support. This work has been supported by the DFG under Contracts SFB 634 and NE 679/2-2 and by the South African NRF.

## References

- [1] Tamii A et al. 2009 *Nucl. Instr. and Meth. A* **605** 326
- [2] Fujita Y et al. 2007 *Phys. Rev. C* **75** 057305
- [3] Matic A et al. 2009 *Phys. Rev. C* **80** 055804
- [4] Dohmann H et al. 2008 *Phys. Rev. C* **78** 041602(R)
- [5] Bäumer C et al. 2003 *Phys. Rev. C* **68** 031303(R)
- [6] Ryezayeva N et al. 2002 *Phys. Rev. Lett.* **89** 272502
- [7] Paar N, Vretenar D, Khan E and Colò G 2007 *Rep. Prog. Phys.* **70** 691
- [8] Heyde K, Neumann-Cosel P and Richter A 2010 *Rev. Mod. Phys.* **82** 2365
- [9] Berg GPA, Foster CC, Stephenson EJ and Davis BF 1994 *IUCF Scientific and Technical Report* p 106
- [10] Fujita H et al. 2007 *Phys. Rev. C* **75** 034310
- [11] Berg GPA 1996 *Proceedings of the 14<sup>th</sup> RCNP OSAKA International Symposium, Nuclear Reaction Dynamics of Nucleon-Hadron Many Body Systems* (Singapore: World Scientific Publishing Co.) p 141
- [12] Fujita H et al. 2002 *Nucl. Instr. and Meth. A* **484** 17
- [13] Fujita H et al. 2001 *Nucl. Instr. and Meth. A* **469** 55